Localized and delocalized vibrations on TiO_2(110) studied by high-resolution electron-energy-loss spectroscopy

G. Rocker and J. A. Schaefer
Physics Department, Montana State University, Bozeman, Montana 59715

W. Göpel*
Institut für Physikalische und Theoretische Chemie der Universität, D-7400 Tübingen, Federal Republic of Germany
(Received 3 October 1983; revised manuscript received 3 January 1984)

Electronic as well as localized and delocalized vibrational losses were studied on TiO_2(110) by electron-energy-loss spectroscopy. Electronic loss features at defect surfaces around 0.8 eV indicate band-gap defect states. In the higher loss-energy range above 3 eV well-known interband transitions were detected, which were found to be sensitive to ion bombardment, but not to the formation of point defects produced by high-temperature pretreatment. Vibronic loss structures are characterized by three different delocalized Fuchs-Kliewer surface phonons at 46, 54, and 95 meV as well as multiple and combination losses thereof. Ion bombardment as well as high-temperature pretreatment reduces their intensities significantly. On defect-free surfaces a shift of all three fundamental frequencies of +2 meV relative to defect surfaces was observed for primary energies below 10 eV. Localized O—H stretching vibrations at 455±1 meV were detected on stoichiometric and defect surfaces after exposure to atomic hydrogen.

I. INTRODUCTION

Studies on rutile TiO_2 surfaces are of great practical importance in the field of gas sensors, catalysts, semiconductor electrodes, photodecomposition of water, etc.[1] In a recent study[2] we have demonstrated that the single-crystal TiO_2(110) surface serves as an ideal prototype surface to study charge-transfer reactions involved in the chemisorption and point-defect formation at the surface. Of particular importance with respect to practical applications is the determination of intrinsic point defects and adsorbed hydrogen species on TiO_2(110).[3]

In this study we investigated the applicability of high-resolution electron-energy-loss spectroscopy (EELS) to identify defects and surface species on TiO_2 from their vibrational structure. This approach to identify surface species has been extremely successful on metal surfaces[4] and covalent semiconductor surfaces.[5] Owing to pronounced contributions from surface optical phonons expected at ionic semiconductor surfaces,[6] the identification of loss features associated with vibrations of surface species is expected to be complicated, particularly in the range of low loss energies. Recent studies on GaAs, InP, GaP, and TiO_2 (110) surfaces[7–9] indicate that these surface optical phonons remain unaltered during different pretreatments of the surface. An exception is a coupling between optical phonons and surface plasmons observed recently on GaAs(110).[7] Surface optical phonons at ionic compound semiconductor surfaces could be treated theoretically by describing the optical properties of solids in terms of an isotropic frequency-dependent dielectric constant[2,10,11] which was assumed to be unaltered by the presence of the surface.

The objective of this work is to investigate TiO_2(110) surfaces without and with intrinsic defects before and after exposure to hydrogen by means of EELS. We find that frequencies as well as intensities of surface optical phonons are influenced by surface defects and that localized absorbate vibrations formed by the interaction of hydrogen with TiO_2(110) surfaces can be identified with EELS. In addition, EELS has been used to characterize electronic states in the band gap which are defect related. These results are important for a future application of EELS to study adsorption phenomena at ionic semiconductor surfaces.

II. EXPERIMENTAL

The experiments were carried out in a Leybold EELS-XPS (electron-energy-loss—x-ray-photoemission spectroscopy) system at a base pressure of $P < 10^{-8}$ Pa. Samples were prepared by repeated argon bombardment (5 min, $E_p = 500$ eV, $i = 3\times10^{-7}$ A, $P_{Ar} = 4\times10^{-5}$ Pa), and subsequent heat treatment at 870 K for 300 sec in $P_{O_2} = 1.3\times10^{-4}$ Pa to restore the surface stoichiometry. For details of the sample preparation see Ref. 2. The surface cleanliness was checked by XPS. The EELS spectra were taken at primary energies between 5.5 and 28 eV and full width at half maximum (FWHM) in the elastic peak between 6.5 and 20 meV in the specular beam direction with $\theta_i = \theta_e = 45°$.

III. RESULTS

The EELS spectra were taken for four different sample pretreatments. The first sample pretreatment led to an ideal stoichiometric surface with negligible concentration of intrinsic defects. In a previous study[2] these defects have been identified as oxygen vacancies at or near the surface. Results from ideal surfaces are indicated by solid

 ©1984 The American Physical Society

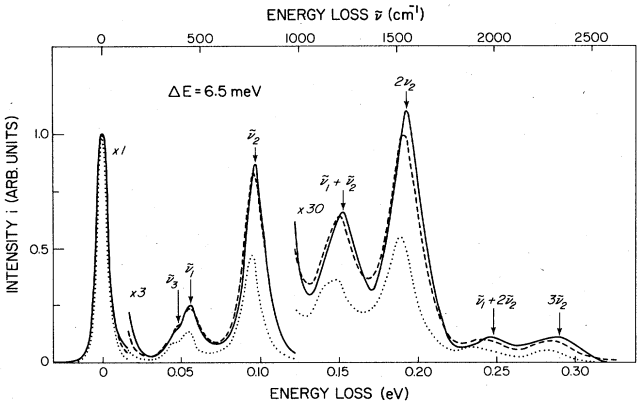

FIG. 1. EELS spectrum of TiO_2(110) after different surface pretreatments. Spectra were taken at a primary energy $E_p = 6.4$ eV with a FWHM of $\Delta E = 6.5$ meV. Solid lines represent results obtained at the stoichiometric surface in the absence of point defects. Dashed lines represent results obtained on surfaces with thermally produced defects.

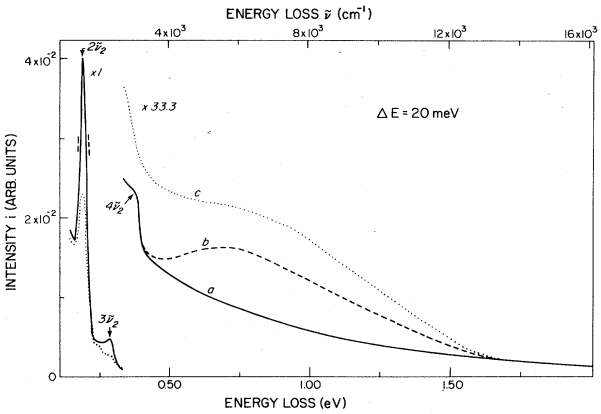

FIG. 3. EELS spectra taken at higher primary energy $E_p = 27.1$ eV with a FWHM $\Delta E = 20$ meV showing the energy range of electronic transitions involving band-gap states. The differently marked lines correspond to different sample pretreatments as described in the caption of Fig. 1. Solid lines represent results from ideal surfaces.

lines in Figs. 1–4. In a second sample pretreatment, surface defects were prepared thermally ($T = 1310$ K, $P_{O_2} = 10^{-8}$ Pa, and $t = 600$ sec), which leads to a nominal defect concentration of 10^{-2} monolayers. Corresponding EELS results are indicated by dashed lines in Figs. 1–4. In a third sample pretreatment, argon bombardment leads to pronounced surface-atom disorders. Results obtained after $P_{Ar} = 4 \times 10^{-5}$ Pa, $t = 600$ sec, and $i = 3 \times 10^{-7}$ A are indicated by dotted lines in Figs. 1–4. The last sample pretreatment consisted of a 1000-L exposure [1 L (Langmuir) $= 10^{-6}$ Torr sec] of atomic hydrogen ($P_{H_2} = 6.7 \times 10^{-4}$ Pa at 300 K) to stoichiometric surfaces during which surface OH groups are formed. We also exposed atomic hydrogen to defect surfaces leading to identical OH features. Exposure of molecular hydrogen did not show any effect on either stoichiometric or defect surfaces.

Figure 1 shows typical results in the range of low loss energies with pronounced peaks from surface optical phonons $\tilde{\nu}_1$, $\tilde{\nu}_2$, $\tilde{\nu}_3$, and with multiple as well as combination losses for the differently prepared samples. In Fig. 2 results obtained from stoichiometric surfaces before and after hydrogen exposure are shown in connection with gain peak features at negative loss energies. Characteristic O–H vibration loss features are observed at 455 meV which can be removed by subsequent thermal treatment at $T \geq 500$ K.

Associated with the formation of point defects and surface-atom irregularities are changes in the electronic transitions which involve gap states. Typical EELS results are shown in Fig. 3 with broad loss features between 0.5 and 1.5 eV. Electronic interband transitions at higher loss energies are shown in Fig. 4. Transitions in this loss-energy range remain basically unaffected if point defects

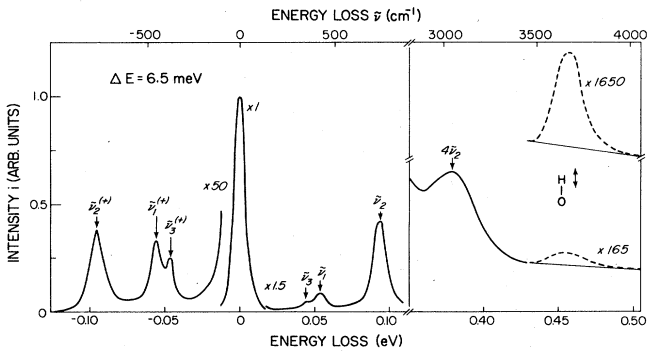

FIG. 2. EELS spectra (obtained for the same experimental conditions as in Fig. 1) shown over a wider energy range which also includes characteristic gain peaks and the effect of hydrogen exposure. Further details are explained in the text.

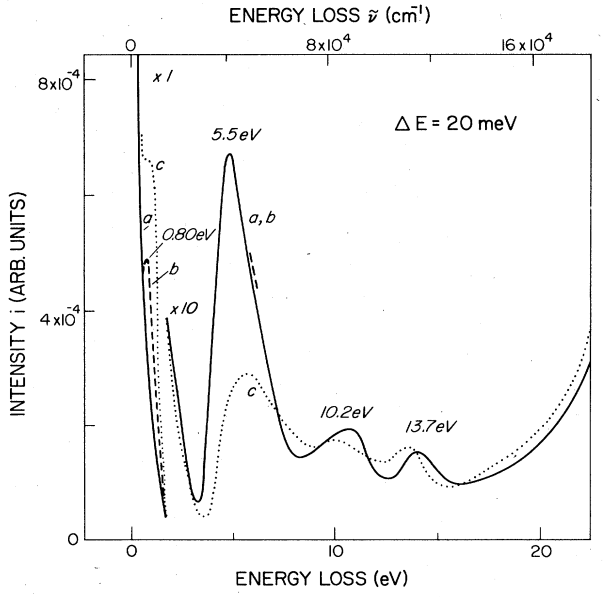

FIG. 4. EELS results obtained under the same experimental conditions and spectrometer parameters as in Fig. 3 in the higher energy range where electronic interband transitions are observed. Further explanations are given in the text.

are formed at stoichiometric surfaces. Significant effects, however, are observed for highly distorted surfaces after argon bombardment (dotted lines).

IV. DISCUSSION

A. Electronic EELS

Before discussing the characteristic vibrational EELS features, we will characterize the differently prepared $TiO_2(110)$ surfaces by means of their different electronic EELS spectra shown in Figs. 3 and 4. A characterization of thermally produced surface defects of $TiO_2(110)$ has been done in a recent paper.[2] These defects are oxygen vacancies associated with two Ti^{3+} surface ions which act as paramagnetic donors. The corresponding EELS transition in Fig. 3 at 0.8 eV is due to a transition between the Ti $3d$ gap state and a maximum of the density of states in the lower energy range of the conduction band.[12] Argon bombardment leads to a broad distribution of electronic states in the gap. Significant changes in the interband electronic transitions (Fig. 4) indicate important changes in the electronic structure of TiO_2 surfaces induced by argon bombardment. Valence-band features are smeared out, and corresponding core-level shifts in the Ti $2p$ and Ti $3p$ peaks indicate partial reduction of titanium even in subsurface regions.[12] Owing to the statistical occurrence of different types of defects after argon bombardment, a detailed description of corresponding geometric and electronic structures is not possible. It is surprising, however, that even after this sample pretreatment the predominant features of the EELS spectra shown in Figs. 1, 3, and 4 remain. This demonstrates the long-range order of delocalized Fuchs-Kliewer phonons to be discussed next.

B. Surface Optical Phonons

The surface optical (Fuchs-Kliewer) phonons observed in our studies can be identified by comparing bulk data[13,14] and a recent theoretical treatment (see Ref. 9 and references therein) with typical results summarized in Table I. The observed surface optical-phonon modes are singly excited surface modes at $\tilde{\nu}_1$, $\tilde{\nu}_2$, and $\tilde{\nu}_3$ as well as combination and multiple excitations of these fundamental modes. The frequencies $\tilde{\nu}_1$ and $\tilde{\nu}_2$ have also been observed in a recent EELS study on $TiO_2(100)$.[9] In our study with better instrumental resolution and signal-to-noise ratio we could also observe the $\tilde{\nu}_3$ mode. It could be determined even more sensitively from the gain feature due to the relative enhancement of lower loss energies according to the Boltzmann distribution, which results in a better separation of $\tilde{\nu}_3$ and $\tilde{\nu}_1$ features in the gain spectrum shown in Fig. 2. For $\tilde{\nu}_2$ in particular we have been able to also observe higher-order multiple losses which show the expected Poisson distribution of intensities[15,16] shown in Fig. 5. The ratio of gain-to-loss intensity shows the expected Boltzmann behavior.[11]

At primary energies above $E_p = 11$ eV, the different sample pretreatments lead to identical values of $\tilde{\nu}_1$, $\tilde{\nu}_2$, and $\tilde{\nu}_3$ as they are listed in Table I. At lower primary energies we observe characteristic shifts of surface optical phonons at stoichiometric surfaces towards higher loss energies. Typical results are shown in Fig. 1 for $E_p = 6.4$ eV. For all three frequencies we find a shift of approximately 2 meV in the fundamental mode, whereas the multiple losses $2\tilde{\nu}_2$, $3\tilde{\nu}_2$, and $4\tilde{\nu}_2$ showed shifts of 2.5, 3, and 3.5 meV for $5.5 \leq E_p \leq 7.0$ eV.

The physical origin of this shift is not quite clear at present. Reduced amplitudes and shifts towards lower loss energies upon defect formation at the surface may qualitatively be understood by damping of the collective vibrational modes in the presence of defect-induced conduction electrons with the frequency of phonons at a defect surface

$$\omega_D = (\omega_s^2 - \kappa^2)^{1/2} \tag{1}$$

for a frequency on the stoichiometric surface ω_s, with $\kappa = \beta/2m^*$, where β is the damping constant, $m^* = 20m_e$ is the effective mass of TiO_2 conduction-band electrons, and m_e is the electron-rest mass. Donor-type point defects in TiO_2 lead to an increase in the free-electron concentration.[20] As an example, from the above-mentioned frequency shift in $\tilde{\nu}_2$ at $E_p = 6.4$ eV we calculate $\beta = 1.7 \times 10^{-16}$ kg sec^{-1} and $\hbar\kappa = 19.6 e_0$ meV for samples with high concentrations of defects.

TABLE I. Summary of surface and bulk optical-phonon frequencies in meV for rutile TiO_2.

Surface data			Bulk data		
Frequency	Mode assignment	Theory[a]	ir-active modes	ir data[b]	INS data[c]
54	$\tilde{\nu}_1$	52.8–56.4	Γ_5^+(LO)	56.8	53.2
95	$\tilde{\nu}_2$	93.8–98.8	Γ_1^-(LO)	100.5	100.6
46	$\tilde{\nu}_3$	46.2–46.3	Γ_5^+(TO)	22.7	23.4
149	$\tilde{\nu}_1+\tilde{\nu}_2$				
141	$\tilde{\nu}_3+\tilde{\nu}_2$				
190	$2\tilde{\nu}_2$				
244	$\tilde{\nu}_1+2\tilde{\nu}_2$				
285	$3\tilde{\nu}_2$				
339	$\tilde{\nu}_1+3\tilde{\nu}_2$				
380	$4\tilde{\nu}_2$				

[a]From Kesmodel *et al.* and references therein (Ref. 9).
[b]Infrared data from Eagles (Ref. 13).
[c]Inelastic neutron scattering data from Traylor *et al.* (Ref. 14).

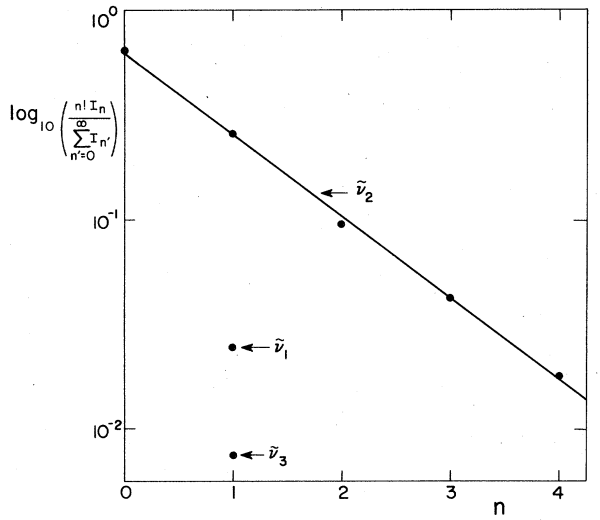

FIG. 5. Poisson distribution of the measured loss intensities for TiO_2(110) Fuchs-Kliewer surface phonons $\tilde{\nu}_2$ at 300 K.

At stoichiometric surfaces, these defects are annealed, and defect-free (sub)surface regions are produced which extend about 1000 Å into the bulk.[2] The dependence of the surface-phonon shift and damping on the primary energy may also be explained by the primary energy dependence of Fuchs-Kliewer phonon amplitudes in subsurface layers. The effective amplitude as a function of distance z from the surface is given by $\exp(-q_{\parallel}|z|)$ with the inverse electron momentum transfer parallel to the surface[8]

$$|\vec{q}_{\parallel}^{-1}| = \frac{|\vec{k}_0|\hbar\omega_s\sin\theta}{2E_p} . \quad (2)$$

Here, $\vec{k}_0$ and E_p are the wave vector and the energy of the incoming electron, respectively, and θ is the scattering angle. For $\tilde{\nu}_2$ we estimate values of $|\vec{q}_{\parallel}^{-1}|$ between 925 and 1934 Å for E_p between 6.4 and 28 eV. Geometric and electronic perturbations in the first few monolayers extend little if compared with $|\vec{q}_{\parallel}^{-1}|$ and the region which contributes to the time-dependent electric field at $E_p > 11$ eV. As a consequence, surface disorder or defects do not affect the observed optical-phonon frequencies at higher primary energies, whereas deviations between ideal and defect surfaces are expected for $|\vec{q}_{\parallel}^{-1}| < 1000$ Å.

The experimentally determined value $\hbar\kappa$ is within experimental error identical with the corresponding plasmon energy frequency of free carriers in these samples of $180e_0$ meV. The latter value was estimated from the concentration of free electrons of 1×10^{19} cm^{-3} and their effective mass. These plasmons couple with Fuchs-Kliewer phonons and cause the above-mentioned damping. Owing to the linewidth of our instrument and the large "background" near the elastic peak resulting from Fuchs-Kliewer phonons we could not resolve plasmon excitations at low energies.

C. Hydrogen-induced adsorbate vibrations

Hydrogen leads to adsorbate vibrations as shown in Fig. 2 which are characteristic of O—H stretch vibrations. In our earlier chemisorption studies on defect surfaces we also found indirect evidence for a Ti-H surface species which only occurs in the presence of surface point defects.[2] These species could not be detected in EELS presumably for two reasons. First, the energy is expected to be at around 260 meV. In this energy range, a large background from contributions of multiple $\tilde{\nu}_2$ excitations are observed. Second, the equilibrium concentration of TiH absorbate complexes is below 10^{-2} monolayers[2] and

TABLE II. Characteristic H and OH vibrational frequencies observed in EELS.

$\hbar\omega$ (meV) Vibrations	TiO_2	Si	Pt	GaAs (Ga site)	GaAs (As site)	InP (In site)	InP (P site)
H	not obs.	257[a] Si(111)	260[b] (ir)	234[c] GaAs(110)	266[c] GaAs(110)	212[d] InP(110) 210[d] InP(100)	297[d] InP(110) 285[d] InP(100)
O—H	455	458[e] Si(100)2×1 456[e] Si(111)7×7	455[f] Pt(100) 431[g] Pt(111)				
OH	52 (calc.)	102[e] Si(100)2×1 100[e] Si(111)7×7	57[f] Pt(100) 53[g] Pt(111)				

[a]Reference 5.
[b]Reference 19.
[c]Reference 7.
[d]Reference 8.
[e]Reference 11.
[f]Reference 17.
[g]Reference 18.

under these conditions it is expected to be below the detection limit of our spectrometer.

The experimentally observed loss in Fig. 2 is found in a frequency range in which O—H vibrations are typically observed on metal and semiconductor surfaces (see Table II). Owing to the large Fuchs-Kliewer phonon background, the corresponding OH vibration could not be resolved. We therefore calculated its value in a simple classical model with the result also shown in Table II. In this calculation we assumed that O—H force constants β(O—H) known from the literature for free O—H radicals [$\hbar\omega$(O—H)$=458e_0$ meV] to a first approximation do not change in the O—H adsorption complex. We also assume that the mass of the surface cations at the adsorption site is large if compared with the mass of oxygen and calculate two eigenfrequencies from

$$\omega(\mathrm{OH})_{\mathrm{ads}}=\frac{1}{2}\left[\frac{\beta}{m_{\mathrm{H}}}+\frac{\beta+K}{m_{\mathrm{O}}}\right] \pm\left[\frac{1}{4}\left[\frac{\beta}{m_{\mathrm{H}}}+\frac{\beta+K}{m_{\mathrm{O}}}\right]^2-\frac{\beta K}{m_{\mathrm{H}}m_{\mathrm{O}}}\right]^{1/2} \tag{3}$$

with K as the force constant of the metal—OH vibration. Assuming $\omega(\mathrm{OH})_{\mathrm{ads}}\ll\omega(\mathrm{O—H})_{\mathrm{free}}$ we find

$$[\omega(\mathrm{OH})_{\mathrm{ads}}]^2=[\omega(\mathrm{O—H})_{\mathrm{free}}]^2-[\omega(\mathrm{O—H})_{\mathrm{ads}}]^2 \tag{4}$$

with $\omega(\mathrm{O—H})_{\mathrm{ads}}$ from the EELS experiment, we determine $\hbar\omega(\mathrm{OH})_{\mathrm{ads}}=52e_0$ meV.

As can be deduced from Table II, the simplifications of our model are also capable of explaining metal—OH and O—H eigenfrequencies at single-crystal Pt surfaces. Owing to the smaller mass of Si the model fails, however, to calculate the corresponding eigenfrequencies on silicon.

V. CONCLUSIONS

We have demonstrated that EELS studies on highly ionic metal oxide surfaces can be used to characterize surface structures by means of the vibrational structure of delocalized surface optical (Fuchs-Kliewer) as well as localized surface vibrations associated with adsorbate formation. Modifications in the intensity and frequency of Fuchs-Kliewer phonons as a function of primary energy may be correlated with the concentration of free electrons near the surface. Localized absorbate vibrations in the higher loss-energy range make possible the determination of hydrogen-atom-derived absorbate species. An experimental tool to detect the latter is essential, e.g., in studying elementary steps of photodecomposition of water on TiO_2. In spite of earlier results and conclusions drawn from those, our results indicate that EELS can indeed be used to study surface reactions on highly ionic semiconductors such as TiO_2 if light atoms such as hydrogen are involved.

ACKNOWLEDGMENTS

Assistance of J. A. Anderson, M. Jaehnig, and D. Frankel, and financial support by the National Science Foundation (NSF) under Grant No. CHE-7916134, Montana State University grant, from the Research Corporation, and from the Fonds der Chemischen Industrie are gratefully acknowledged. The work was carried out at the Center for Research in Surface Science and Submicron Analysis (CRISS), an NSF Regional Instrumentation User Facility at Montana State University in Bozeman, MT.

*To whom correspondence should be sent.

[1]See, e.g., A. Jujishima and K. Honda, Nature (London) **238**, 37 (1972); V. E. Henrich, Prog. Surf. Sci. **9**, 143 (1979); *Basic Research Opportunities for Lasting Fuel Gas Supplies Report from Workshop at Texas A&M University, 1981,* edited by C. A. Rodenberger *et al.* (Gas Research Institute, Chicago, 1982); *Solar Energy Conversion: Solid State Physics Aspects, Vol. 31 of Topics in Applied Physics,* edited by B. O. Seraphim (Springer, Berlin, 1981), and references therein.

[2]W. Göpel, G. Rocker, and R. F. Feierabend, Phys. Rev. B **28**, 3427 (1983).

[3]M. L. Knotek, Surf. Sci. **91**, L17 (1980); **101**, 334 (1980).

[4]H. Ibach and D. L. Mills, *Electron Energy Loss Spectroscopy and Surface Vibrations* (Academic, New York, 1982).

[5]See, e.g., H. Froitzheim, in *Electron Spectroscopy for Surface Analysis,* edited by H. Ibach (Springer, Berlin, 1977).

[6]R. Fuchs and K. L. Kliewer, Phys. Rev. **140**, A2076 (1965).

[7]H. Lüth, Surf. Sci. **126**, 126 (1983), and references therein.

[8]L. H. Dubois and G. P. Schwartz, Phys. Rev. B **26**, 794 (1982).

[9]L. L. Kesmodel and J. A. Gates, Phys. Rev. B **23**, 489 (1981).

[10]D. L. Mills, Prog. Surf. Sci. **8**, 143 (1977), and references therein.

[11]H. Ibach, H. Wagner, and D. Bruchmann, Solid State Commun. **42**, 457 (1982).

[12]W. Göpel *et al.*, Surf. Sci. **139**, 333 (1984).

[13]D. M. Eagles, J. Phys. Chem. Solids **25**, 1243 (1964).

[14]J. G. Traylor, H. G. Smith, R. M. Nicklow, and M. K. Wilkinson, Phys. Rev. B **3**, 3457 (1971).

[15]A. A. Lucas and M. Sunjic, Prog. Surf. Sci. **2**, 2 (1972).

[16]E. Evans and D. L. Mills, Phys. Rev. B **5**, 4126 (1972).

[17]H. Ibach and S. Lehwald, Surf. Sci. **91**, 187 (1980).

[18]G. B. Fisher and B. A. Sexton, Phys. Rev. Lett. **44**, 683 (1980).

[19]J. P. Candy, P. Foulloux, and M. Primet, Surf. Sci. **72**, 167 (1978).

[20]A. von Hippel, F. Kalnajs, and W. B. Westphal, J. Phys. Chem. Solids **23**, 779 (1962).